

POWER CLASS TIME-FREQUENCY REPRESENTATIONS: INTERFERENCE GEOMETRY, SMOOTHING, AND IMPLEMENTATION

Antonia Papandreou-Suppappola

Franz Hlawatsch

G. Faye Boudreaux-Bartels

Dept. of Electrical/Computer Eng.
University of Rhode Island
Kingston, RI 02881 USA
antonia@ele.uri.edu

INTHFT, Vienna Univ. of Technology
Gusshausstrasse 25/389
A-1040 Vienna, Austria
fhlawats@email.tuwien.ac.at

Dept. of Electrical/Computer Eng.
University of Rhode Island
Kingston, RI 02881 USA
boud@ele.uri.edu

ABSTRACT

The κ th power class (PC_κ) of quadratic time-frequency representations (QTFRs) is specifically suited for the multiresolution analysis of signals passing through systems whose dispersion characteristic is approximately f^κ . This paper considers several aspects of PC analysis important in applications. We discuss the geometry of PC auto terms and cross terms, and we propose new PC QTFRs that attenuate cross terms via smoothing. We describe the implementation of PC QTFRs via warping techniques. Finally, simulation results demonstrate the advantages of PC analysis.

1. INTRODUCTION

Quadratic time-frequency representations (QTFRs) are powerful tools for time-varying signal analysis [1-3]. Different QTFR classes exist that are best suited for analyzing signals with certain properties. For example, affine class QTFRs are covariant to time-frequency (TF) scalings and constant (i.e. nondispersive) time shifts and can be used for constant-Q TF analysis [1, 4, 5]. More generally, power class (PC) QTFRs are covariant to TF scalings and power-dispersive time shifts and can be used for analyzing signals passing through dispersive systems [6-8].

This paper addresses several aspects of PC QTFRs important in applications: the geometry of PC auto and cross terms, new PC QTFRs that use TF smoothing to reduce cross terms, the implementation of PC QTFRs, and simulations demonstrating the advantage of PC TF analysis.

We start with a brief review of the PCs. Let $X(f)$ denote the Fourier transform of a signal. The κ th power class (PC_κ), $\kappa \neq 0$, consists of QTFRs $T_X^{(\kappa)}(t, f)$ covariant to TF scalings and to dispersive time shifts corresponding to "power" group delays [6-8]. That is, if $X(f)$ is scaled and power time-shifted, $Y(f) = |a|^{-\frac{1}{2}} X(\frac{f}{a}) e^{-j2\pi c \xi_\kappa(f/f_r)}$, then $T_Y^{(\kappa)}(t, f) = T_X^{(\kappa)}(a(t - c\tau_\kappa(f)), \frac{f}{a})$ where $\xi_\kappa(b) = \text{sgn}(b)|b|^\kappa$ is the power phase function whose derivative yields the power group delay $\tau_\kappa(f) = \frac{\kappa}{f_r} |f/f_r|^{\kappa-1}$, $\text{sgn}(b)$ is +1 if $b > 0$ and -1 if $b < 0$, $a \in \mathbb{R} \setminus \{0\}$, $c \in \mathbb{R}$, and $f_r > 0$ is a fixed reference frequency. PC_κ QTFRs are specifically suited for the multiresolution analysis of signals passing through dispersive systems with power-function group delays $\tau_\kappa(f) \propto f^{\kappa-1}$. Such group delay laws are simple models for dispersive environments such as in underwater acoustic signal analysis.

This work was supported in part by NUWC contract N66604-96-C-A336, by ONR grant N00014-96-1-0350, and by FWF grant P10531-ÖPH.

Any PC_κ QTFR can be written as [6, 8]

$$T_X^{(\kappa)}(t, f) = \int_{-\infty}^{\infty} \int_{-\infty}^{\infty} W_X^{(\kappa)}(t', f') \cdot \psi_T \left(\xi_\kappa \left(\frac{f}{f_r} \right) \left[\frac{t}{\tau_\kappa(f)} - \frac{t'}{\tau_\kappa(f')} \right], -\xi_\kappa \left(\frac{f'}{f} \right) \right) dt' df' \quad (1)$$

where $\psi_T(c, b)$ is a 2-D kernel characterizing $T^{(\kappa)}$. The κ th power Wigner distribution (WD_κ), $W_X^{(\kappa)}(t, f)$, is a prominent member of the PC_κ defined as

$$W_X^{(\kappa)}(t, f) = \left| \frac{f}{\kappa} \right| \int_{-\infty}^{\infty} X \left(f \xi_{\frac{1}{\kappa}} \left(1 + \frac{\beta}{2} \right) \right) X^* \left(f \xi_{\frac{1}{\kappa}} \left(1 - \frac{\beta}{2} \right) \right) \cdot e^{j2\pi \frac{t}{\kappa} \beta} \left| 1 - \frac{\beta^2}{4} \right|^{\frac{1-\kappa}{2\kappa}} d\beta \quad (2)$$

$$= \int_{-\infty}^{\infty} \rho_X^{(\kappa)} \left(\frac{t}{\tau_\kappa(f)} + \frac{\zeta}{2} \right) \rho_X^{(\kappa)*} \left(\frac{t}{\tau_\kappa(f)} - \frac{\zeta}{2} \right) e^{-j2\pi \xi_\kappa \left(\frac{f}{f_r} \right) \zeta} d\zeta \quad (3)$$

where $\rho_X^{(\kappa)}(c) = \int_{-\infty}^{\infty} X(f) \sqrt{|\tau_\kappa(f)|} e^{j2\pi c \xi_\kappa(f/f_r)} df$.

The PC_κ generalizes the affine class [4, 5] since the affine class is the PC_κ with $\kappa = 1$. Any PC_κ QTFR, $T_X^{(\kappa)}(t, f)$, can be derived from a corresponding affine class QTFR, $T_X^{(A)}(t, f) = T_X^{(1)}(t, f)$, by a "power warping" [6-9],

$$T_X^{(\kappa)}(t, f) = T_{W_\kappa X}^{(A)} \left(\frac{t}{f_r \tau_\kappa(f)}, f_r \xi_\kappa \left(\frac{f}{f_r} \right) \right) \quad (4)$$

with the power-warped version of the signal $X(f)$ given by

$$(W_\kappa X)(f) = \frac{1}{\sqrt{|\kappa|}} \left| \frac{f}{f_r} \right|^{\frac{1-\kappa}{2\kappa}} X \left(f_r \xi_{\frac{1}{\kappa}} \left(\frac{f}{f_r} \right) \right). \quad (5)$$

The WD_κ in (2), (3) is the power-warped version of the Wigner distribution, which is the WD_κ for $\kappa=1$. Other PC_κ QTFRs include the powergram [6, 8], the Bertrand P_κ -distributions [5], and the power Bertrand distribution [8].

2. INTERFERENCE GEOMETRY

The WD_κ satisfies many desirable properties [6, 8] and provides excellent TF concentration. In particular, the WD_κ of a "power impulse," $I_c^{(\kappa)}(f) = \sqrt{|\tau_\kappa(f)|} e^{-j2\pi c \xi_\kappa(f/f_r)}$, is a Dirac ridge centered along the power group delay curve,

$$W_{I_c^{(\kappa)}}^{(\kappa)}(t, f) = |\tau_\kappa(f)| \delta(t - c\tau_\kappa(f)), \quad (6)$$

and the WD_κ of a complex sinusoid, $L_{f_0}(f) = \delta(f - f_0)$, is a Dirac ridge at f_0 ,

$$W_{L_{f_0}}^{(\kappa)}(t, f) = \delta(f - f_0). \quad (7)$$

Similar TF concentration properties are exhibited by the Bertrand P_κ -distributions [5, 10].

Like other QTFRs, the PC_κ QTFRs contain quadratic cross or interference terms in the case of multicomponent or complicated monocomponent signals (cf. [1, 3, 11]). The geometrical properties of auto and cross terms are important in applications, especially with a view towards attenuating cross terms by means of smoothing. We shall investigate the basic “interference geometry” of the PC_κ by discussing the interference geometry of the WD_κ (see also Section 4). The WD_κ of a two-component signal $X(f) = X_1(f) + X_2(f)$,

$$W_X^{(\kappa)}(t, f) = W_{X_1}^{(\kappa)}(t, f) + W_{X_2}^{(\kappa)}(t, f) + C_{X_1, X_2}^{(\kappa)}(t, f),$$

consists of two *auto terms*, $W_{X_i}^{(\kappa)}(t, f)$, ($i = 1, 2$), and one *cross term*, $C_{X_1, X_2}^{(\kappa)}(t, f) = 2\text{Re}\{W_{X_1, X_2}^{(\kappa)}(t, f)\}$, which is twice the real part of the cross WD_κ of $X_1(f)$ and $X_2(f)$ (defined as in (2) with X replaced by X_1 and X^* replaced by X_2^*). We shall first consider two basic examples.

Two power impulses. For the sum of two power impulses, $X_i(f) = I_{c_i}^{(\kappa)}(f) = \sqrt{|\tau_\kappa(f)|} e^{-j2\pi c_i \xi_\kappa(f/f_r)}$, ($i = 1, 2$), the auto terms are $W_{X_i}^{(\kappa)}(t, f) = |\tau_\kappa(f)| \delta(t - c_i \tau_\kappa(f))$ (cf. (6)), and the cross term is

$$C_{X_1, X_2}^{(\kappa)}(t, f) = 2 |\tau_\kappa(f)| \delta\left(t - c_{12} \tau_\kappa(f)\right) \cos\left(2\pi \zeta_{12} \xi_\kappa\left(\frac{f}{f_r}\right)\right)$$

with $c_{12} = \frac{c_1 + c_2}{2}$ and $\zeta_{12} = c_1 - c_2$. The cross term is an oscillatory Dirac ridge along the power group delay curve

$$t = c_{12} \tau_\kappa(f) = c_{12} \frac{\kappa}{f_r} \left| \frac{f}{f_r} \right|^{\kappa-1} \quad \text{with } c_{12} = \frac{c_1 + c_2}{2}. \quad (8)$$

It oscillates in the frequency direction with f -dependent oscillation “frequency”

$$\mu_{12}(f) = \frac{d}{df} \left\{ \zeta_{12} \xi_\kappa\left(\frac{f}{f_r}\right) \right\} = \zeta_{12} \tau_\kappa(f) \quad (9)$$

which is seen to be proportional to the parameter difference $\zeta_{12} = c_1 - c_2$. More generally, if the signal components are power time-shifted versions of a given signal $X_0(f)$, i.e. $X_i(f) = X_0(f) e^{-j2\pi c_i \xi_\kappa(f/f_r)}$, ($i = 1, 2$), then the WD_κ auto terms are $W_{X_i}^{(\kappa)}(t, f) = W_{X_0}^{(\kappa)}(t - c_i \tau_\kappa(f), f)$ and the cross term is given by

$$C_{X_1, X_2}^{(\kappa)}(t, f) = 2 W_{X_0}^{(\kappa)}\left(t - c_{12} \tau_\kappa(f), f\right) \cos\left(2\pi \zeta_{12} \xi_\kappa\left(\frac{f}{f_r}\right)\right).$$

Two complex sinusoids. For $X_i(f) = L_{f_i}(f) = \delta(f - f_i)$, ($i = 1, 2$), the auto terms are Dirac ridges at the signal frequencies, $W_{X_i}^{(\kappa)}(t, f) = \delta(f - f_i)$ (cf. (7)), and the cross term is given by

$$C_{X_1, X_2}^{(\kappa)}(t, f) = 2 \left| \tau_\kappa\left(\frac{f_1 f_2}{f_1 + f_2}\right) \right|^{1/2} \delta(f - f_{12}) \cos(2\pi \nu_{12} t)$$

with

$$f_{12} = f_r \xi_\kappa \left(\frac{\xi_\kappa(f_1/f_r) + \xi_\kappa(f_2/f_r)}{2} \right) \quad (10)$$

and

$$\nu_{12} = \frac{\xi_\kappa(f_1/f_r) - \xi_\kappa(f_2/f_r)}{\tau_\kappa(f_{12})}. \quad (11)$$

This is a Dirac ridge at the “average frequency” f_{12} , oscillating in the time direction with oscillation frequency ν_{12} .

Generalization. Combining the above results, it is possible to formulate a general characterization of the WD_κ interference geometry. If there are auto terms around two

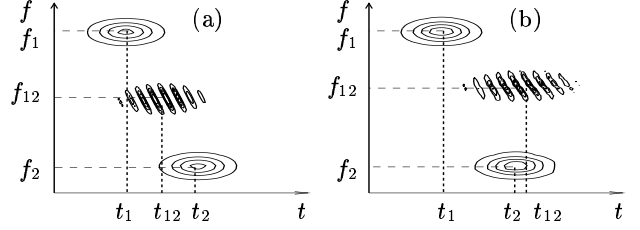


Fig. 1. WD_κ of the sum of two Gaussian signals. (a) Wigner distribution, WD_1 , with cross term located around the mean TF point $(t_{12}, f_{12}) = (\frac{t_1+t_2}{2}, \frac{f_1+f_2}{2})$, (b) WD_3 with cross term located around $(t_{12}, f_{12}) = (\frac{1}{2}(\frac{t_1}{f_1} + \frac{t_2}{f_2}) f_{12}^2, (\frac{f_1^3+f_2^3}{2})^{1/3})$.

TF points (t_1, f_1) and (t_2, f_2) (see Fig. 1), then there will be a corresponding cross term around the TF point (t_{12}, f_{12}) , where f_{12} is defined in (10). In order to find t_{12} , we note that the cross term must be located somewhere around the line $f = f_{12}$ (see (10)) and also somewhere around the power group delay curve $t = c_{12} \tau_\kappa(f)$ where $c_{12} = \frac{c_1 + c_2}{2}$ (see (8)). Here, c_1 and c_2 are defined by the power group delay curves that pass through the TF points (t_1, f_1) and (t_2, f_2) , respectively, i.e., $t_1 = c_1 \tau_\kappa(f_1)$ and $t_2 = c_2 \tau_\kappa(f_2)$. This results in $t_{12} = c_{12} \tau_\kappa(f_{12})$ where $c_{12} = \frac{1}{2} \left[\frac{t_1}{\tau_\kappa(f_1)} + \frac{t_2}{\tau_\kappa(f_2)} \right]$ and $\tau_\kappa(f_{12}) = \frac{\kappa}{f_r} \left| \frac{\xi_\kappa(f_1/f_r) + \xi_\kappa(f_2/f_r)}{2} \right|^{1-1/\kappa}$. Furthermore, the cross term around (t_{12}, f_{12}) oscillates in the time direction with local oscillation frequency $\nu_{12} = \frac{\xi_\kappa(f_1/f_r) - \xi_\kappa(f_2/f_r)}{\tau_\kappa(f_{12})}$ (see (11)), and in the frequency direction with local oscillation frequency (measured along the group delay curve $t = c_{12} \tau_\kappa(f)$) $\mu_{12}(f_{12}) = \zeta_{12} \tau_\kappa(f_{12})$ (see (9)). Hence, around (t_{12}, f_{12}) the cross term allows a local approximation

$$C_{X_1, X_2}^{(\kappa)}(t, f) \approx A \cos\left(2\pi[\mu_{12}(f_{12}) f - \nu_{12} t] + \phi\right),$$

with a local amplitude A and a local phase ϕ . Note that this interference geometry of the WD_κ generalizes that of the Wigner distribution [11], which is reobtained when $\kappa=1$. More generally, the interference geometry of the PC_κ generalizes that of the affine class (i.e. the PC_κ with $\kappa=1$) [10]. In particular, the interference geometry of the Bertrand P_κ -distributions, which are members of both the affine class and the PC_κ , is discussed in [10].

3. POWER CLASS SMOOTHING

In many applications, it is important to reduce QTFR cross terms by means of smoothing. The PC_κ expression (1) can be interpreted as smoothing the WD_κ if the kernel $\psi_T(c, b)$ is a smooth (lowpass) function. Rewriting (1) as

$$T_X^{(\kappa)}(t, f) = \int_{-\infty}^{\infty} \int_{-\infty}^{\infty} W_X^{(\kappa)}(c' \tau_\kappa(f'), f') \cdot \psi_T\left(\xi_\kappa\left(\frac{f}{f_r}\right) \left[\frac{t}{\tau_\kappa(f)} - c' \right], -\xi_\kappa\left(\frac{f'}{f_r}\right)\right) |\tau_\kappa(f')| dc' df',$$

the smoothing is seen to consist of two components: (i) the c' integration corresponds to a smoothing in the time direction which is stronger when the smoothing kernel $\psi_T(c, b)$ is broader with respect to c , and (ii) the f' integration corresponds to a smoothing along the power group delay curve $t = c' \tau_\kappa(f')$ (with c' considered fixed) which is stronger when $\psi_T(c, b)$ is broader with respect to b . For a given $\psi_T(c, b)$, the smoothing characteristic also depends on the TF analysis point (t, f) in $T_X^{(\kappa)}(t, f)$. In the following, we discuss three particular PC QTFRs that implement smoothing.

Powergram. The *powergram* (the squared magnitude of the power wavelet transform [6]) has a smoothing kernel

$$\psi_T(c, b) = W_H^{(\kappa)} \left(-\tau_\kappa(f_r \xi_\perp^\kappa(b))c, -f_r \xi_\perp^\kappa(b) \right)$$

that is a warped WD_κ of an analysis wavelet $H(f)$. Hence, the two smoothing components are not independent, and the overall amount of smoothing cannot be made arbitrarily small. The powergram is analogous to the spectrogram in Cohen's class [1–3, 11], and to the scalogram in the affine class [1, 3, 4]; the scalogram is reobtained when $\kappa=1$.

Power smoothed pseudo Wigner distribution. A simple smoothing kernel that allows unrestricted choice of the two smoothing components is the separable function

$$\psi_T(c, b) = g(c)H(b),$$

where $g(c)$ and $H(b)$ are 1-D lowpass functions. This results in a new PC_κ member which we call the κ th *power smoothed pseudo Wigner distribution* (PSPWD $_\kappa$). The PSPWD $_\kappa$ is the power-warped version of the affine smoothed pseudo Wigner distribution [4], which is reobtained when $\kappa=1$. The two kernel factors $g(c)$ and $H(b)$ control the two smoothing components independently: a broader $g(c)$ yields more smoothing in the time direction whereas a broader $H(b)$ yields more smoothing along the power group delay curves. The PSPWD $_\kappa$ allows a continuous passage from the WD_κ (case of no smoothing) to the powergram (case of strong smoothing). The proof of this result is similar to that for the Wigner distribution and scalogram case given in [4].

It can be shown that the PSPWD $_\kappa$ can be constructed as follows. (i) The WD_κ in (3) is first calculated with $\rho_X^{(\kappa)}(c)$ formally replaced by the locally windowed version

$$\rho_X^{(\kappa)}(c) w \left(\xi_\kappa \left(\frac{f}{f_r} \right) \left(c - \frac{t}{\tau_\kappa(f)} \right) \right) e^{j2\pi \xi_\kappa \left(\frac{f}{f_r} \right) \left(c - \frac{t}{\tau_\kappa(f)} \right)}$$

(i.e. $\rho_X^{(\kappa)}(c)$ is multiplied by the “window” $w(c) e^{j2\pi c}$ scaled by $\xi_\kappa(\frac{f}{f_r})$ and shifted by $c=t/\tau_\kappa(f)$). The resulting *power pseudo Wigner distribution* can be expressed as

$$\begin{aligned} \widetilde{W}_X^{(\kappa)}(t, f) &= \frac{1}{|\xi_\kappa(f/f_r)|} \int_{-\infty}^{\infty} W_X^{(\kappa)} \left(\frac{\tau_\kappa(f')}{\tau_\kappa(f)} t, f' \right) \\ &\cdot H \left(-\xi_\kappa \left(\frac{f'}{f} \right) \right) |\tau_\kappa(f')| df' \end{aligned}$$

where $H(b)$ is the Fourier transform of $h(c)=w(\frac{c}{2})w^*(-\frac{c}{2})$. The smoothing kernel of $\widetilde{W}_X^{(\kappa)}(t, f)$ is $\psi_T(c, b)=\delta(c)H(b)$.

(ii) The power pseudo Wigner distribution above is then smoothed with respect to time to yield the PSPWD $_\kappa$

$$\text{PSPWD}_X^{(\kappa)}(t, f) = \left| \frac{f}{\kappa} \right| \int_{-\infty}^{\infty} g \left(\frac{f}{\kappa} (t - \hat{t}) \right) \widetilde{W}_X^{(\kappa)}(\hat{t}, f) d\hat{t}.$$

Power-warped smoothed pseudo Bertrand P $_0$ -distribution. We propose a further new PC_κ member, the power-warped version of the smoothed pseudo Bertrand P $_0$ -distribution [12], which can be expressed as

$$\begin{aligned} \text{SPP}_{0X}^{(\kappa)}(t, f) &= \int_{-\infty}^{\infty} S_X^{(\kappa)} \left(\frac{t}{f_r \kappa \tau_\perp(f_r \lambda(u))}, f \xi_\perp^\kappa(\lambda(u)) \right) \\ &\cdot S_X^{(\kappa)*} \left(\frac{t}{f_r \kappa \tau_\perp(f_r \lambda(-u))}, f \xi_\perp^\kappa(\lambda(-u)) \right) g(u) du. \end{aligned}$$

Here, $\lambda(u) = u/(1 - e^{-u})$ [5], $g(u)$ is a lowpass smoothing function [12], and $S_X^{(\kappa)}(t, f)$ is the κ th power wavelet transform defined in [6]. This QTFR provides smoothing both in

the time and in the frequency directions, and allows efficient computational schemes using the power wavelet transform. The smoothed pseudo Bertrand P $_0$ -distribution [12] is reobtained when $\kappa=1$.

4. IMPLEMENTATION AND SIMULATION RESULTS

Implementation. The discrete implementation of PC_κ QTFRs can be based on the warping relations (4) and (5), which allows the use of existing efficient algorithms for computing affine class QTFRs [13]. This implementation is similar conceptually to the implementation of hyperbolic class QTFRs [14] proposed in [15, 16]. It consists of (i) a power-law frequency warping of the signal $X(f)$ according to (5), (ii) computation of the affine QTFR of the warped signal, $T_{\mathcal{W}_\kappa X}^{(A)}(t, f)$, and (iii) a nonlinear TF coordinate transform according to (4), $(t, f) \rightarrow \left(\frac{t}{f_r \tau_\kappa(f)}, f_r \xi_\kappa \left(\frac{f}{f_r} \right) \right)$.

For the discrete implementation of Step (i), the discrete version of the signal's Fourier transform (FT), $X[l]$ ($l=0, 1, \dots, L-1$), with frequency sample spacing Δf , is first interpolated (upsampled) by a factor u , yielding the FT samples $X'[l']$ ($l'=0, 1, \dots, uL-1$). Next, discrete warped-frequency locations are computed according to (5) such that uniform sampling of the warped-frequency axis is achieved; these discrete warped-frequency locations are given by $f_m = f_r \xi_\perp^\kappa \left(\frac{m \Delta v}{f_r} \right)$ ($m=0, 1, \dots, M-1$), where Δv is the frequency sample spacing of the warped FT computed such that $|f_{m+1} - f_m| \leq \Delta f, \forall m$, and M is the number of warped FT samples required to represent the entire frequency domain. The FT value at each warped-frequency location f_m is obtained by linear interpolation of the closest neighbors in the upsampled FT $X'[l']$. This gives a discrete warped-frequency FT $Y[m]$ ($m=0, 1, \dots, M-1$). In order to avoid time-aliasing effects in the subsequent computation of the affine QTFR, the warped-frequency FT $Y[m]$ is finally interpolated (upsampled) to bandlimit the FT to one quarter of the sampling rate, yielding $Y'[m']$ ($m'=0, 1, \dots, M'-1$) where $M'=2M$.

In Step (ii), a discrete-time, discrete-frequency version of the affine QTFR $T_{Y'}^{(A)}(t, f)$ [4, 13] is computed for the warped-frequency signal $Y'[m']$.

Step (iii) computes the warped TF locations $(t_n, f_i) = \left(\frac{n/f_r}{f_r \tau_\kappa(f_i)}, f_i \right)$ where $f_i = f_r \xi_\kappa \left(\frac{i \Delta f}{f_r u} \right) / \left(\frac{\Delta v}{f_r} \right)$ ($n, i=0, 1, \dots, L-1$), such that uniform 2-D sampling in the warped TF domain is achieved, and subsequently calculates the corresponding sample values $T_{Y'}^{(A)}(t_n, f_i)$ using linear 2-D interpolation.

We note that a generalized discussion of the overall discrete implementation technique can be found in [15].

Simulation results. We applied the discrete implementation outlined above to analyze the sum of two power impulses, $I_c^{(\kappa)}(f) = \sqrt{|\tau_\kappa(f)|} e^{-j2\pi c \xi_\kappa(f/f_r)}$, for $\kappa=3$. Fig. 2 compares an “ideal” TF representation (sum of the WD_3 of the individual signal components) with the Wigner distribution (WD), and the 3rd power WD_3 and PSPWD_3 . Note that the power parameter $\kappa=3$ of the WD_3 and the PSPWD_3 is *matched* to that of the power impulses. The WD is not matched to the power impulses, displaying cross terms between the impulses and “inner” interference terms [3, 11] below the bottom power impulse (see also Fig. 3b). The WD_3 has better TF concentration of auto and cross terms, without inner interference terms. The PSPWD_3 removes the cross terms present in the WD_3 with only moderate TF concentration loss.

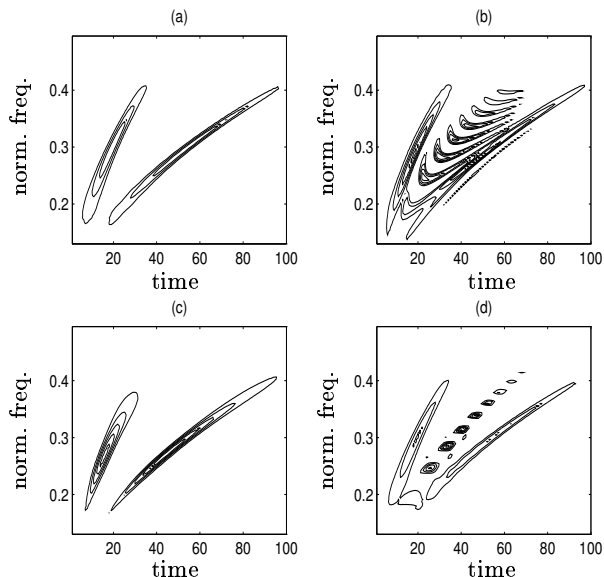


Fig. 2. TF analysis of the sum of two power impulses with $\kappa=3$: (a) “Ideal” QTFR, (b) WD, (c) PSPWD₃, (d) WD₃.

In the next example, the two power impulses changed to have $\kappa=4$, but we continue to analyze this signal with PC₃ QTFRs (which are now “mismatched” since the power parameter of the signal, $\kappa=4$, is different from that of the PC QTFRs used, $\kappa=3$). Fig. 3 compares the WD and the affine smoothed pseudo WD (both members of the affine class) with the WD₃ and the PSPWD₃. Both the WD and the WD₃ contain significant cross terms, with the WD₃ cross terms showing better TF concentration than the WD cross terms. These cross terms are better suppressed in the PSPWD₃ than in the affine smoothed pseudo WD; furthermore, the PSPWD₃ shows less resolution loss since the PSPWD₃ smoothing is better matched to the geometry of the signal and cross terms. Thus, the PC₃ QTFRs still perform better than conventional affine (i.e., PC κ with $\kappa=1$) QTFRs even though signal-QTFR mismatch occurs.

5. CONCLUSION

The recently proposed power class (PC) QTFRs [6–8] are useful for the multiresolution analysis of signals passing through dispersive systems. This paper considered various aspects of PC analysis that are important in practical applications, such as the geometry of PC QTFR auto and cross terms, new PC QTFRs that attenuate cross terms by smoothing, and the implementation of PC QTFRs using warping techniques. We finally presented simulation results demonstrating the advantages of PC analysis.

Acknowledgment

We would like to thank P. Gonçalves for the software used for computing the affine smoothed pseudo WD.

6. REFERENCES

- [1] P. Flandrin, *Temps-fréquence*. Paris: Hermès, 1993.
- [2] L. Cohen, *Time-Frequency Analysis*. Prentice-Hall, 1995.
- [3] F. Hlawatsch and G. F. Boudreaux-Bartels, “Linear and quadratic time-frequency signal representations,” *IEEE Signal Processing Mag.*, vol. 9, pp. 21–67, April 1992.
- [4] O. Rioul and P. Flandrin, “Time-scale energy distributions: A general class extending wavelet transforms,” *IEEE Trans. Signal Processing*, vol. 40, pp. 1746–1757, July 1992.
- [5] J. Bertrand and P. Bertrand, “A class of affine Wigner functions with extended covariance properties,” *J. Math. Phys.*, vol. 33, pp. 2515–2527, 1992.

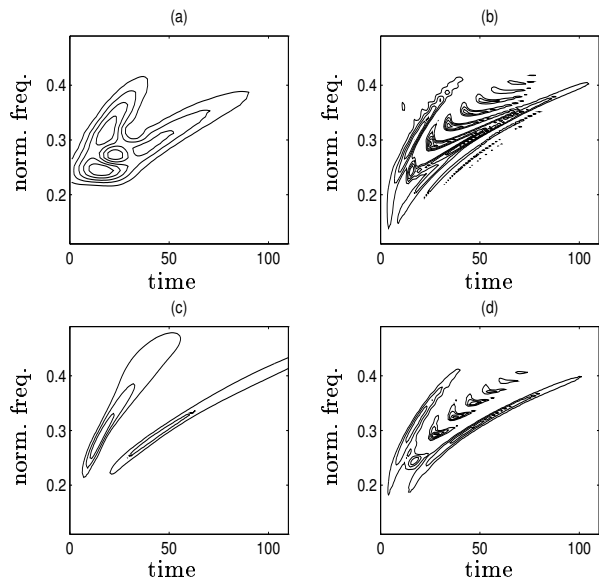


Fig. 3. TF analysis of the sum of two power impulses with $\kappa=4$: (a) Affine smoothed pseudo WD, (b) WD, (c) PSPWD₃, (d) WD₃. Note that the κ parameters of the signal and the PC₃ QTFRs are different.

- [6] F. Hlawatsch, A. Papandreou, and G. F. Boudreaux-Bartels, “The power classes of quadratic time-frequency representations: A generalization of the affine and hyperbolic classes,” *Proc. 27th Asilomar Conf.*, (Pacific Grove, CA), pp. 1265–1270, Nov. 1993.
- [7] A. Papandreou, F. Hlawatsch, and G. F. Boudreaux-Bartels, “A unified framework for the scale covariant affine, hyperbolic, and power class time-frequency representations using generalized time-shifts,” *Proc. IEEE ICASSP-95*, (Detroit, MI), pp. 1017–1020, May 1995.
- [8] A. Papandreou-Suppappola, *New classes of quadratic time-frequency representations with scale covariance and generalized time-shift covariance: Analysis, detection, and estimation*. PhD thesis, Univ. of Rhode Island, RI, May 1995.
- [9] R. G. Baraniuk and D. L. Jones, “Unitary equivalence: A new twist on signal processing,” *IEEE Trans. Signal Processing*, vol. 43, pp. 2269–2282, Oct. 1995.
- [10] P. Flandrin and P. Gonçalves, “Geometry of affine time-frequency distributions,” *Appl. Comput. Harm. Anal.*, Jan. 1996.
- [11] F. Hlawatsch and P. Flandrin, “The interference structure of the Wigner distribution and related time-frequency signal representations,” in *The Wigner Distribution—Theory and Applications in Signal Processing* (W. Mecklenbräuker, ed.), Elsevier, to be published.
- [12] P. Gonçalves and R. G. Baraniuk, “A pseudo-Bertrand distribution for time-scale analysis,” *IEEE Signal Processing Letters*, vol. 3, pp. 82–84, March 1996.
- [13] J. P. Ovarlez, J. Bertrand, and P. Bertrand, “Computation of affine time-frequency distributions using the fast Mellin transform,” *Proc. IEEE ICASSP-92*, (San Francisco, CA), pp. 117–120, 1992.
- [14] A. Papandreou, F. Hlawatsch, and G. F. Boudreaux-Bartels, “The hyperbolic class of quadratic time-frequency representations, Part I,” *IEEE Trans. Signal Processing*, vol. 41, pp. 3425–3444, Dec. 1993.
- [15] K. G. Canfield and D. L. Jones, “Implementing TFRs for non-Cohen classes,” in *Proc. 27th Asilomar Conference*, (Pacific Grove, CA), pp. 1464–1468, Nov. 1993.
- [16] V. S. Praveenkumar, *Implementation of hyperbolic class time-frequency distributions and removal of cross-terms*. MS thesis, Univ. of Rhode Island, RI, 1995.